ENGINEERING SCIENCES

Infrared reflectance techniques applied to silica particles diameter determination - theoretical and experimental data

RACHEL F. MAGALHÃES, ALEXANDRA H. DE BARROS, MARCIA M. TAKEMATSU, ALAN PASSERO, MILTON F. DINIZ, JAIRO SCIAMARELI & RITA C.L. DUTRA

Abstract: Silica is a versatile material employed in different applications fields including aerospace, especially for rocket engines thermal protections. It is known that particles diameter causes variations in the material properties, and the best-known methods for diameter determination in general consist of several steps in sample preparation such as drying, sieving and the determination of the refractive index according different methods. On the other hand, Fourier transform infrared spectroscopy techniques (FT-IR), in reflectance mode, related to the particle size, are less used for this type of determination. Moreover, methodologies in the near infrared region (NIR) are even less explored. Therefore, the aim of this paper is to present a FTIR methodology for diffuse reflectance (DRIFT) in the middle infrared region (MIR) and reflectance analysis in near infrared region (NIRA) for the determination of the particle diameter on silica samples. Both methodologies showed good results. As proven by a test sample analysis, NIRA methodology indicated better precision. Furthermore, considering small and intermediated particle sizes, a tendency towards smaller errors for the absorbance measurements of the samples was found, consistently with the available literature results.

Key words: Particle diameter, DRIFT, MIR, NIRA, silica.

INTRODUCTION

Silica, chemical compound silicon dioxide (SiO_2), is the most abundant naturally occurring mineral on planet Earth and therefore it is an interesting material for several scientific researches. Silica is a fundamental product in industrial abrasive and polish processes (Tang et al. 2020, Xu et al. 2019), in special coatings (Sriram et al. 2020, Lu et al. 2019, Söz et al. 2015) in electronic optics (Sharma et al. 2018, Butov et al. 2002), in ferro-silicon manufacture (Boldyrev et al. 2019, Siddique & Chahal 2011), in rubber formulations (Sattayanurak et al. 2020), concrete (Chen et al. 2017), besides being an essential and indispensable material for glass manufacture (Karnati et al. 2020, Elsayed et al. 2019, Vukcevich 1972).

In aeronautical applications some research has been carried out on silica aerogel (Bheekhun et al. 2013), but although this material shows excellent properties, having lower density, thermal conductivity, refractive index and dielectric constant than any other solid, a large scale production for the aerospace industry generates problems, such as the extensive and time-consuming procedures involved in the synthesis of aerogels and the high manufacturing cost.

The processing of specific quality silica occurs from different types of silicates. These include colloidal, fumed, fused, high purity crushed silica, silica gel and precipitated silica (Bulatovic 2015).

Colloidal silica is mainly used as a high temperature binder for silicon tablets, polishing and precipitated silica (Arai et al. 2019, Tweddle et al. 2019). Known as one of the most widely used polishing abrasives in chemical-mechanical planarization (CMP) (Lei et al. 2019), it has low hardness, low maximum particle size (around 130nm) and stable chemical properties. Consequently, it promotes the minimization of the scratches and damage amount to surfaces, as well as high efficiency and quality at CMP (Shi et al. 2014).

Resulting from the pyrogenic manufacture by combustion of silicon tetrachloride in an oxygen-hydrogen flame (Barthel et al. 1996), fumed silica consists of highly porous and fractal nanoparticles aggregates (Amoabeng et al. 2020). Due to its ability to improve polymers mechanical properties (Kong et al. 2019), as well as to reinforce composites (Gürgen 2019, Rajaee et al. 2019), fumed silica supports different applications.

For instance, since the major contribution of the nano-sized fillers is supporting the filler/matrix interaction surface, Gürgen 2019 used the fumed silica particles in the ultra-high molecular weight polyethylene (UHMWPE) matrix to enhance the wear performance of the base material. Rajaee et al. 2019 investigated the microstructure and mechanical properties of glass fiber reinforced unsaturated polyester (GFRP) composites modified by styrene-butadiene rubber (SBR) and fumed silica. The addition of fumed silica nano-filler improved tensile, flexural and impact strength, tensile and flexural modulus but reduced the elongation at break.

Fused silica, glass composed of amorphous silica (Schill et al. 2018), results from the fusion of high-quality silica sand in electric arc and resistance furnaces. Since fused silica is an important material in optical engineering (Dai et al. 2019, Campbell et al. 2004), many studies focused on the minimization of surface damage

(Tan et al. 2020). This converted silica can also be used as an electronic encapsulant (Phua et al. 2018).

High purity crushed silica is the product obtained from silica sand or soft and friable rocks after being processed in order to eliminate impurities (Martins 2016). Another possibility of obtaining high purity crushed silica is through microfluidic-inclusion fracture, using microwave pretreatment (Buttress et al. 2019). Present in most soil original materials, quartz is the most common form of crystalline silica that can be found (Gutiérrez-Castorena & Effland 2010).

Silica gel is known as one of the most studied materials for water vapor adsorption (Freni et al. 2019). Composed of a vast interconnected microscopic pores network, it contains polymerized silica particles (Sahu & Singh 2019). These particles surfaces are covered with silanol groups which are hydrophilic in nature (Basrur & Sabde 2016). Basrur & Sabde (2016) also emphasize that its properties depend on the agglomeration extension and on the primary particle size. Volume, pore size distribution, surface area and surface chemistry are adjusted by optimizing the synthesis parameters (Alaei et al. 2013).

Due to the difficulty in the supply of raw materials to produce carbon black, precipitated silica had a great increase as an alternative material (Da Silva 2013). For instance, in the production of light-coloured rubber with reinforced properties (Zafarmehrabian et al. 2012). Precipitated silica is obtained from the neutralization of a sodium silicate alkaline solution with sulfuric acid. This treatment produces a sol-gel composed of sodium sulfate and insoluble which is separated and processed for production. Reaction conditions such as reagents addition rate, concentration, agitation, temperature and pH are determinants for the precipitated silica properties, mainly particularly for particle size.

References about the use of silica and the effect of its particle size on polymeric formulations properties, those required for aerospace applications, can be found in the literature (Halim et al. 2017, Bray et al. 2013, Alaei et al. 2013, Gomes 1993). Therefore, the development of methodologies to determine the particle diameter of this material is important to predict properties.

Halim et al. (2017) investigated a particulate composite material prepared by adding three different sizes of silica aerogel particles to an unsaturated polyester resin, with 30% of fixed volume fraction. The more porous is the area of the larger silica aerogel particles, the lower are the degradation rate and the thermal conductivity of the sample. Nevertheless, the addition of silica aerogel in the resin reduced the matrix tensile modulus, where the use of smaller particle size resulted in greater toughness than that obtained with larger particle size.

Several properties of rubbers are affected by silica addition. For example, in the aerospace field, rubbers such as polymers based on ethylene-propylene-diene monomer (EPDM) (Paiva & Garbelotto 2006) and butadiene-acrylonitrile copolymer (NBR) (Gomes 1993) that are used as thermal protections for rocket engines.

Silica as a filler in EPDM rubber formulations is employed in both aerospace and automotive industries, among others (Paiva & Garbelotto 2006). Most polymers formed from EPDM are amorphous and must be reinforced to achieve adequate properties for the intended project. The usage of silica as a reinforcement filler in rubber formulations has proved to be an alternative of great interest in the market for carbon black replacement. NBR rubber requires addition of silica or carbon black so that properties such as tensile strength, tear strength and abrasion resistance can reach

adequate values, in order to meet each project specific conditions (Gomes 1993). The purpose is to develop artifacts with different coloring type, with characteristics similar to those obtained by black colored products manufactured using carbon black.

This scenario points to the importance of using silica, as well as the knowledge of its particles size in polymeric formulations. To predict any new manufactured product properties, it is necessary to discuss methods for particle diameter determination and the development of new methodologies in the scientific field, especially for silica which is a versatile material in the industrial field.

In the two last decades, particle diameter determination has been carried out by different instrumental techniques such as granulometric analysis (Shimadzu 2020, Wagner & Aranha 2007), X-ray diffraction (XRD) (Mcnab et al. 2017); scanning electron microscopy (SEM) and transmission electron microscopy (TEM) (Tian et al. 2020, Bahrani et al. 2018), as well as Fourier transform infrared spectroscopy (FT-IR) (Osswald & Fehr 2006).

To obtain data about larger and smaller particle sizes in the suitable elaboration of particle size distribution curves, two methods can be used: Mie Scattering Theory and Fraunhofer diffraction theory, also known as Fraunhofer Approximation (Shimadzu 2020, Wagner & Aranha 2007, Nai-Ning et al. 1992).

Mie scattering theory is extremely complex and more difficult to understand than Fraunhofer diffraction theory. It requires a more complex programming and a fast computer processor. In addition, in some cases, information about the refractive index is not known, not even its average value which is required in Mie Theory. For this reason, Fraunhofer Approximation was more used in the past and it is still widely applied. (Shimadzu 2020).

Many available laser particle size equipment based on the Fraunhofer diffraction technique are widely used for particle size measurement. However, errors may occur when this type of equipment is used to determine small particle dimensions. In this way, significant improvement could be reached out when classical Mie's scattering theory is applied in the small size particle range. Based on this idea, a Fraunhofer diffraction and Mie scattering (FAM) laser particle sizer has been evaluated and studied by Nai-Ning et al. 1992. Experiments carried out by them using the combination of theories suggested better results in the large and small size particle ranges measurement.

On the other hand, if Mie Theory is applied to very large particle size, an accumulated miscalculation phenomenon occurs and inaccurate results can be obtained, while the Fraunhofer Approximation is more suitable to get a more accurate calculation result for the light intensity distribution pattern. For this reason, both Fraunhofer diffraction theory and Mie scattering theory are currently applied together to calculate the light intensity distribution pattern to ensure that a wide measurement range is covered (Shimadzu 2020).

Mie theory describes the particle size measurement as homogeneous spheres of arbitrary size. For non-spherical particles, it considers the equivalent spherical diameter by volume-weight.

Spectroscopy is a science aimed at the investigation and measurement of spectra generated when materials absorb electromagnetic radiation. As a product of the excitation of molecular vibrations after infrared (IR) beam incidence through the sample, FTIR spectrum provides information on functional groups and its chemical structures (Smith 1979).

During the last decades, infrared spectroscopy in the MIR and NIR regions has proved to be versatile in several aspects since there is available a significant number of method developments in the literature addressing different types of materials (polymer, soil, drugs, tissues, and industrial raw materials) (Dudek et al. 2021, Ozaki 2012). It has also shown remarkable progress in its use in applied science, whether in polymers (Carvalho et al. 2021, Magalhães et al. 2020, Azevedo et al. 2018, Mello et al. 2018) or in inorganic micromolecules (Pinto et al. 2018). In the aerospace field, the progress was concentrated in the thermal protection compositions and catalysts (Campos et al. 2010, Tagliaferro et al. 2006).

NIR spectra arise from molecular bonds vibrational energy transitions with a high dipole moment (Cabassi et al. 2015). The spectrum complexity is marked by the appearance of overtones (multiples of the fundamental MIR bands) and combination bands (addition or subtraction of fundamental MIR bands). These types of absorption bands arise from the interaction of two or more vibrations that happen simultaneously, which makes it difficult to assign bands (Osborne 2000).

Due to this difficulty, a variety of spectral pre-treatments, such as Savitzky-Golay smoothing, is applied to complement and enable a better analysis of the spectrum obtained (Ozaki 2012). Although, where there are no overlapping bands and a band intensity variation can be detected reflecting the sample concentration, treatments as chemometric algorithms are not required (Mello et al. 2018).

In addition, FTIR analysis allows sampling depth degree variation, in micrometers, using reflection/reflectance and photoacoustic spectroscopy. For instance, FTIR allows measurement at different paths of the sample in ATR mode depending of refractive index of the IRE (internal reflection element) crystal used and/or the incident angle. This capability

stimulates researches, in different IR spectrum regions, of other spectra obtaining ways for compounds analysis, such as transflectance in the near infrared (NIRA) region (Magalhães et al. 2020 and references therein).

Diffuse reflectance (DRIFT) occurs on not entirely flat surfaces, with a continuous or fragmented (powder) substrate. In this reflectance process, the incident beam penetrates the sample surface interacting with the matrix. After partial absorption and multiple scattering, the beam returns to the sample surface. Since there is no optical contact problem, external reflectance experiments, such as those obtained by DRIFT, show an advantage over internal reflectance, e.g., attenuated total reflection (ATR), (Magalhães et al. 2020, Ferrão 2001). The light path cannot be controlled and varies according to particle size and refractive index (Ferrão 2001).

Near infrared reflectance analysis (NIRA) can use an accessory to collect data from diffuse reflectance spectra of solid and powder samples (Hopkinson et al. 2018). It involves a direct analysis without the need for prior sample preparation. For this reason, this technique is classified as non-destructive, non-invasive, with high penetration in the sample (Williams & Norris 2001), and it is also considered a low-cost, fast and safe analysis (Zhao et al. 2018).

Besides optical path length variations and crystalline forms presence, sample particle diameter size is a property that also directly affects NIR spectrum (Ramalho et al. 2019, Roggo et al. 2007). This influence is also proven by Gao et al. (2017) when observing that morphology and pigment particle size of the studied composite play an important role in light scattering efficiency. As reported by Sheppard et al. (2019), another element that influences the absorption band intensity is the strong spectral contrast between the absorption species, e.g.,

transparent minerals such as quartz when mixed with opaque high-absorption minerals, such as magnetite.

Considering these characteristics, there is a motivation to evaluate the particle diameter determination by IR, by reflection, reflectance or transflectance, also considering that in DRIFT analysis, particle size must be considered through the Kubelka-Munk relationship (Dai et al. 2018). Given that the sample particle size affects light scattering, it is important to establish an adequate particle size determination methodology, whether in the MIR or NIR region.

Initially, in order to gather data to develop new methodologies for silica particles size determination by FT-IR, the material characteristics and the instrumental techniques, which can be used as references were explored. Then, characteristics of FTIR spectra obtaining modes such as diffuse reflectance (DRIFT) and transflectance (NIRA) were presented and discussed.

In addition, Table I shows publications that include different instrumental techniques and FTIR analysis conditions. All the references are related to silica compounds characterization for influence evaluation and particle size or diameter determination, with further discussion of some FTIR publications.

Regarding the studies related to infrared (IR) spectroscopy analysis and silica particle size as well, it is possible to highlight some data on analytical bands (Osswald & Fehr 2006).

Osswald & Fehr (2006) applied transmission infrared spectroscopy to obtain information on silica solutions structures and their sol-gel processes. They mention that silica gel is a very important material in sol-gel technology, and usually, tetraethyl orthosilicate (TEOS) is used as a precursor in this area. Gel formation process of inorganic silica solutions is quite different from TEOS gel formation, which is due to monomers

polymerization. On the other hand, the gel formation process of inorganic silica solutions is due to dense particles condensation, with particle diameters of a few nanometers. Most of the information acquired in the IR analysis was derived from the main silica band at ~ 1070 (Si-O-Si stretch). In both silica solutions and silica gel, there are nearby bands at about 1040 and 1027 which are attributed to the vibration modes. The intensity of these bands contains information about the silica particles size in liquid solutions. The authors concluded that FTIR spectroscopy is a useful method for the determination of alkaline silica solution particle sizes. As the particle size is correlated with the solution alkaline content, this band intensity could also be used to determine the alkali content. However, it was observed that this was only possible for solutions with the same silica concentration. Particle size information was limited to the nanometric particles between 2 and 6 nm, specifically for smaller particles. For larger particles, it was observed an interference in the analytical band intensity measurement by oth(*) dynamic light scattering (DLS); centrifugal liquid sedimentation (CLS); atomic force microscopy (AFM); particle tracking analysis (PTA); the other acronyms have already been cited in the text.

Although good results were obtained in their study (Osswald & Fehr 2006), transmission, by capillary film analysis (a thin liquid film, without use of spacer, prepared between two polyethylene foils) was the chosen spectral mode. Thus, if other conditions such as the use of a spacer or relative band (band intensity ratio) for thickness control had been considered, more accurate data could have been achieved.

The relative band is composed of an analytical band and a reference band to eliminate the interference of the sample thickness variation (the Lambert-Beer law),

which can cause errors in the measurement of the bands intensity.

The literature (Kestens et al. 2016) also mentions the development of a new reference material. It is a certified material whose purpose is to control the quality of different silica nanoparticles size analyzing methods. The material consists of an aqueous suspension of a nanoparticle silica mixture of different particles sizes and origin. The used methods were DLS, CLS, SEM, TEM, AFM, and PTA and measurements were carried out in several competent laboratories. A uniform interpretation problem was observed in all the participants in the interlaboratory test carried out. The value assignment was a challenge due to the metrological concepts not always being interpreted uniformly across all participant laboratories. But at the end of experiments, the results obtained confirmed that the term "particle size" does not sufficiently describe the exact quantity that is measured in the different methods. It was observed that the equivalent diameter values of some measurement methods differ, and that some data only coincide because of their relatively large uncertainty. For a reliable particle size comparison, it has been proposed that a more detailed specification of the measurand "particle size" could be made, including the physical principles of the measurement method and the procedure followed for data analysis. Therefore, it can be concluded that one should not give particle size measurement data without associating all the conditions used to obtain that specific values.

The number of entries in Table I reflects the low volume of scientific articles on silica particles diameter determination. The existence of a gap in the scientific database is highlighted, and consequently, the need for further study in this field. Although good results have been found in publications on particle size influence

Table I. Literature data on instrumental techniques used in influence evaluation and particle size determination.

Authors / year	Analyzed sample	Instrumental technique or method	Average size	Spectrum obtaining mode / sample preparation	Remarks
Domínguez et al. (2020)	Silica (nanoparticle)	Sedimentation	50-200 nm	-	Relative error: 10% (95% of the data explained by the methodology)
Sharma & Polizos (2020)	Silica (hollow or mesoporous particles)	SEM, TEM	≤ 1 µm	-	FT-IR spectroscopy is referred to qualitative surface characterization
Stach et al. (2020)	Silica (quartz), calcite, dolomite	FT-IR	1-5 µm	Transmission / ATR / DRIFT / as received	DRIFT is more susceptible to particle size than transmission. Unlike XRD, smaller particle sizes show an increase in signal
Kestens et al. (2016)	Silica (nanoparticle - certified reference material)	DLS, CLS, SEM, TEM, AFM, PTA(*)	20-80 nm	-	-
Osswald & Fehr (2006)	Silica (silica gel - solution)	FT-IR	2-6 nm	Transmission / liquid film between polyethylene sheets	Methodology was limited to smaller particles. For larger particles, it was observed an interference in the analytical band intensity measurement by other neighboring bands.

(*) dynamic light scattering (DLS); centrifugal liquid sedimentation (CLS); atomic force microscopy (AFM); particle tracking analysis (PTA); the other acronyms have already been cited in the text.

or diameter determination, it is observed that few of these studies employ FT-IR spectroscopy, especially in NIR which is less applied to inorganic compounds (Ozaki 2012). Usually, spectra are collected in DRIFT and transmission modes. In addition, the best results are for smaller particle sizes. Whereas for larger particles band interference and high errors were also found.

Given this scenario, the purpose of this paper is to evaluate FT-MIR/DRIFT and NIRA methodologies for silica particles diameter determination using different analytical bands

with the purpose of finding greater measurement precision than those observed in conventional methodologies such as granulometric analysis, which is used as a reference in the present study.

MATERIALS AND METHODS

Materials and equipment

Seven silica samples provided by different suppliers, coded as: MSS 500, Chiffonsil -5, Oristar Silica 7, Silica Balloon BA4, Silica HDK N20, HPTLC plate silica and TLC plate silica were analyzed.

The MSS 500, OriStar Silica 7 and Silica HDK N20 samples were supplied with the diameter D50 (μm) data: 3.28, 5.93 and 16.46, respectively, obtained by Fraunhofer Approximation. For the other samples, D50 values were determined by two granulometric analysis methods, Fraunhofer Approximation and/or Mie theory.

D50 is the corresponding particle size when the accumulated percentage reaches 50%. D50 is also called median particle diameter or median particle size. For example, for a powder sample with D50 = 5 μm, it means there are 50% particles larger than 5 μm and 50% particles smaller than 5 μm.

For the granulometric analysis, the Mastersizer particle analyzer equipment from Malvern Instruments was used. For FTIR analyzes, two PerkinElmer spectrophotometers were used, Spectrum One model for DRIFT/MIR, and FTIR/NIR Frontier for NIRA accessory.

Methodology development

Two instrumental methods were used: granulometric analysis and Fourier Transformed Infrared Spectroscopy (FT-IR). Particle diameter median values D50 of silica samples obtained by granulometric method were used as reference for the development of calibration curves involving FTIR analytical bands absorbance values (A) versus silica particle diameter D50 values to compose the FTIR methodologies (DRIFT/MIR and NIRA). In the DRIFT methodology developed, the samples were not diluted with KBr in order to reduce the time of analysis.

Granulometric analysis conditions

Granulometric data were obtained by two methods: Fraunhofer Approximation and Mie theory. The analyzes were performed in an aqueous mean using water as a dispersant. The results represent the average of nine runs. The refractive index used in the Mie method was set to 1.5, which is the average value for silica.

FTIR analysis conditions

The spectral ranges explored were: 4000 to 400 (MIR) and 10,000 to 4,000 (partial NIR range), with a 4 resolution, gain 1 and 40 scan average. Two spectral modes were used: DRIFT and NIRA with the samples analyzed as received. Since bands intensity in reflectance spectra considers the particle size, the purpose of this analysis was to check the existence of a relationship between particle diameter D50 and the intensity of characteristic silica bands (Ferrão 2001).

In DRIFT (MIR) analysis, the analytical band evaluated falls at around 1060, representative of (Smith 1979). The baseline used for suitable measurement of the height or intensity of the analytical band at 1060 cm-1 was: 1282 cm-1 (initial point) to 492 cm-1 (end point). This analytical band is assigned to stretching of SiO in SiO2 (Smith 1979).

Although the NIR bands between 4000 - 5500 can be assigned to fundamental MIR bands combination (sum) (Goddu 1960), another probable allocation for the band at 5268 might be referred to the fourth band overtone at 1060. The 4440 band is probably assigned to the fundamental silica bands combination. The baselines used were: 5403 to 4916 (band at 5268) and 4708 to 4245 (band at 4440).

According to Lambert-Beer's law (Smith 1979), the equation A = bc, which rules quantitative infrared analysis, was used to determine the calibration or analytical curves, relating the relative bands with the D50 obtained by the Fraunhofer Approximation:

where: A= absorbance

ε = molar absorptivity (characteristic of absorption)

b = thickness

c = concentration (in this case, D50)

the thickness (b) of the analyzed sample will be the same in the sample spectrum, and when dividing one band absorbance by the other, b cancels out.

$$\frac{A_1}{A_2} = \frac{\varepsilon_1 b c_1}{\varepsilon_2 b c_2}$$

In NIRA analysis, the bands at 5268 and 4440 (NIR region) were evaluated to constitute a relative band A_{4440}/A_{5268} that includes silica characteristic bands. Relative band usage aims to theoretically cancel the thickness effect.

The result of the analytical band (A_{1060} or relative A_{4440}/A_{5268}) height measurement (intensity) for each sample represents the median of five values. The errors involved were calculated according to the non-parametric statistical method (Hórak & Vítek 1978) (Equations 1 to 3), successfully used for FTIR spectroscopic data in different studies (Janzen et al. 2021, Carvalho et al. 2021, Ferreira et al. 2020, Rigoli et al. 2019, Azevedo et al. 2018). The methodology error (%), considered as the median of the relative errors, (Dutra & Soares 1998) was also calculated. According to Hórak & Vítek (1978), for small set of data, the median is used instead of the average.

$$\hat{\sigma} = K_R \times R \tag{1}$$

where $\hat{\sigma}$ is the standard deviation, R represents the difference between the highest and the lowest absorbance values and KR equals 0.430 for 5 measures (Hórak & Vítek 1978).

$$\hat{\sigma}_{\hat{\mu}} = \frac{\hat{o}}{\sqrt{n}} \tag{2}$$

$$RD_{(\%)} = \frac{\hat{\sigma}_{\hat{\mu}}}{\mu} \times 100 \tag{3}$$

where n represents the total number of measures, RD is the relative deviation and μ is the median absorbance value.

FTIR methodology effectiveness verification

To verify the effectiveness of the developed FTIR methodology, a sample with D50 around 5 μm was analyzed by another analytical research laboratory and the sample was coded as "sample A". NIRA analysis which proved to be the most suitable for this determination, especially for smaller D50 samples between 3-6 μm, were conducted. This analysis meets the criteria in the literature for different methodologies (Stach et al. 2020, Osswald & Fehr 2006).

The NIRA band intensity ratio / was used with its corresponding calibration curve. With the same procedure, five aliquots samples analyzed as received were analyzed under the same conditions and the median value was applied to the equation. According to the methodology used to determine the curve, the errors involved in the measurement were also evaluated (Hórak & Vítek 1978).

RESULTS AND DISCUSSION

Granulometric analysis

Table II shows the determined particle diameter values for the different silica samples, by Fraunhofer Approximation method. The other samples were supplied with the diameter D50 (μm) data. The acronym D10 and D90 means that 10% and 90% of the sample, by volume, are below the measured values, respectively. Only D50 has been investigated in this study, since it is the median value, most used and most representative of the particle distribution.

Table III shows the particle diameter values for the different silica samples, by Mie Theory. The other samples were supplied with the diameter D50 (μm) data.

Table II. Granulometric analysis data for silica samples - Fraunhofer diffraction theory.

Sample	D10 (µm)	D50 (median) (µm)	D90 (µm)
Chiffonsil -5	1.66	4.87	11.50
Silica Balloon BA4	2.12	6.13	16.10
HPTLC plate silica	4.20	6.94	12.50
TLC plate silica	4.95	11.40	26.40

Table III. Granulometric analysis data for silica samples – Mie Theory.

Sample	D10 (µm)	D50 (median) (µm)	D90 (µm)
Chiffonsil -5	2.84	6.03	10.90
Silica Balloon BA4	3.63	7.05	16.90

The data obtained for the same samples analyzed by two granulometric methods (Table II and III) are relatively close.

Although Mie Theory is considered more accurate, it was observed as a result of the granulometric curves data that, apparently, there are greater errors in the Mie theory than in the Fraunhofer Approximation. The samples, analyzed by two methods, with smaller particle sizes show the smallest errors in the Fraunhofer method (Table IV). Then, with the aim of elaborating the FTIR methodology, the Fraunhofer Approximation granulometric method was chosen to be used for the reference D50 values.

Developed FTIR methodology characteristics

It is known that the greater the number of points on a calibration curve, greater the measurement accuracy probability (Horák & Vítek 1978). Initially, some tests were carried out to use as many numbers of silica samples with known D50 as possible. However, not all samples yielded a good linearity. As some provided samples had

close D50 values, the analytical band intensity values (height) fell within the experimental error, it showed less accuracy.

Based on this fact, sample systems with analytical and/or relative bands were tested for the methodologies in MIR and NIR regions in order to obtain better results. Adequate results are those that responded to the Lambert-Beer law plotting a calibration curve with an R (correlation coefficient or coefficient of Pearson correlation) value closer to 1 (greater linearity) and, consequently, greater value. The is a statistical measure of how close the data is to the fitted regression line. It is also known as the coefficient of determination. The higher the value, the greater the number of data explained by the developed methodology and the lower the error, meaning a greater precision. The same interpretation can also be found in a recent paper (Carvalho et al. 2021). Using the obtained calibration curve, other D50 values can be calculated with relatively good precision.

Qualitative analysis DRIFT/MIR and NIRA

In diffuse reflectance analysis (DRIFT), the incident infrared beam penetrates the sample surface interacting with the matrix. After partial absorption and multiple scattering, the beam returns to the sample surface. This process happens several times with the sample particles, and consequently, the radiation is attenuated. Therefore, this radiation provides both qualitative

Table IV. D50 errors (%) comparison of Fraunhofer Approximation and Mie Theory methods for silica samples.

Sample	D50 error Fraunhofer approximation (%)	D50 error Mie theory (%)
Chiffonsil -5	0.842	2.52
Silica Balloon BA4	0.418	2.65
Silica Sicosil 175	2.14	2.30

and quantitative information about the sample (Ferrão 2001, Fuller & Griffts 1978).

The Kubelka-Munk function can relate diffuse reflectance spectra with sample concentration. The reflectance spectrum is transformed into a format similar to an absorbance spectrum, linear to the sample concentration, is suitable for quantitative analysis. For this reason, the Kubelka-Munk function (Equation 4) is known as the Lambert-Beer Law of reflectance spectroscopy (Ferrão 2001, Fuller & Griffts 1978). The intensity values employed in the calculations and later reported in Table V are reported in absorbance unit, as mentioned in the section "Methodology development".

$$F(R\infty) = (1-R\infty)2/2R\infty = k/s \qquad (4)$$

where $R\infty$ is the sample reflectance for infinite depth, k is the sample absorption coefficient, which is proportional to the concentration, and s is the sample scattering coefficient.

Significant deviations from the theory occur at $R\infty < 0.6$. Then, it is recommended to study different dilution of sample to be measured against a blank standard solution which has a known scattering coefficient at different wavelengths. But there is some criticism in this concept and this dilution could not be effective.

The scattering coefficient determines the incident light interaction extent with the sample before the radiation returns to the surface. To a certain extent, *s* controls the depth at which the light penetrates the sample. The lower the *s* value, the higher the $F(R\infty)$ value. However, there is a limit to this behavior, as it is only valid for the particles that effectively spread the incident radiation. Consequently, the particle size effect displaces the baseline. This behavior becomes very distinct at wavelengths of great absorption by the sample. For example, in two different samples with the same composition, but with different particle sizes, there is greater reflectance of smaller (finer) particles. Also, specular reflection effects are minimized on a surface composed of smaller particles (Korte 1988).

In diffuse reflectance, the specular reflection can also be observed, which occurs at the interface present between the air and matrix surface, causing distortions in certain regions of the spectrum. The size of the particles, the existing void, and the degree of compaction between the particles are some reasons that can interfere significantly in the spectral response. Moreover, another factor that can impact the result of spectra in diffuse reflection is the quality of sample preparation, the standardization of the procedure can ensure also better results.

A proper quantification in powder samples depends on the effective penetrating power, that must be large enough to provide a representative spectrum of the sample.

Another spectrum obtaining mode and specific to the near infrared region (NIRA) involves both transmission and reflectance process, whereas in DRIFT occurs only the reflectance mode. The reflectance is applied in solid samples and transflectance in liquids. Also, it can be applied for both qualitative and quantitative evaluations. The NIRA accessory is used for transreflection analysis in the near infrared (Perkinelmer 2011).

No chemometric treatment (Azevedo et al. 2018, Mello et al. 2018) was applied to the data since no band overlapping occur and increase of the absorption intensity is clearly related to the increase in concentration.

Since the characteristics mentioned before ensured the adequacy for powder samples quantitative analysis, the silica samples with different diameters D50 were evaluated by both methodologies, DRIFT in MIR region and NIRA in NIR region.

Figures 1 (a-f) and 2 (a-e) show the qualitative assay of some analyzed samples by DRIFT/MIR and NIRA spectral modes respectively. The interpretation of these spectra aims to demonstrate that the choice of analytical bands was based on the bands that showed increases in the transmittance signal, especially those observed in the samples composed of smaller particles.

In DRIFT/MIR methodology, bands around 850 and 1060 cm-1 apparently show an intensity variation with increasing D50. In order to better analyze smaller diameter samples (majority in this research) the band at 1060 cm-1, with the highest intensity, was chosen as the main one. For NIRA methodology, the band at 4440 cm-1 was chosen as the analytical band, and, the one found at 5268 cm-1, as a reference, as already explained.

Sicosil silica and Silica HDK N20 samples were only used for the analytical band qualitative evaluation. Because of their high D50 value, they were not used for quantitative DRIFT/MIR measurements. It is known that for samples with particle sizes larger than the wavelength, the absorbance generally decreases while increasing particle size. This happens because the reflectance fraction increases with the particle size increase (Torrent & Barron
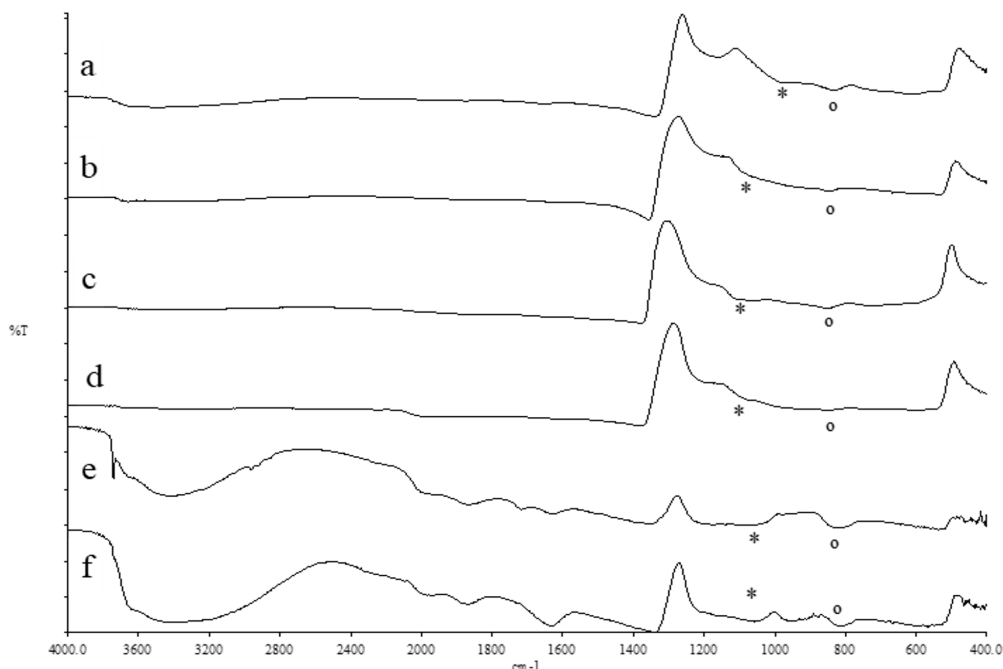
Figure 1. DRIFT / MIR spectra of silica samples of different D (50) (μm), measured by Fraunhofer. Marked bands: 850 cm-1 (0) and 1060 cm-1 (*): a) MSS 500 (3.28); b) Chiffonsil-5 (4.87); c) Oristar Silica 7 (5.93); d) Silica Balloon BA4 (6.13); e) Silica HDK N20 (16.46); f) Silica Sicosil 175 (67.8). The displacement (distortion) of the band at 1060 cm-1 may be due to specular reflection.
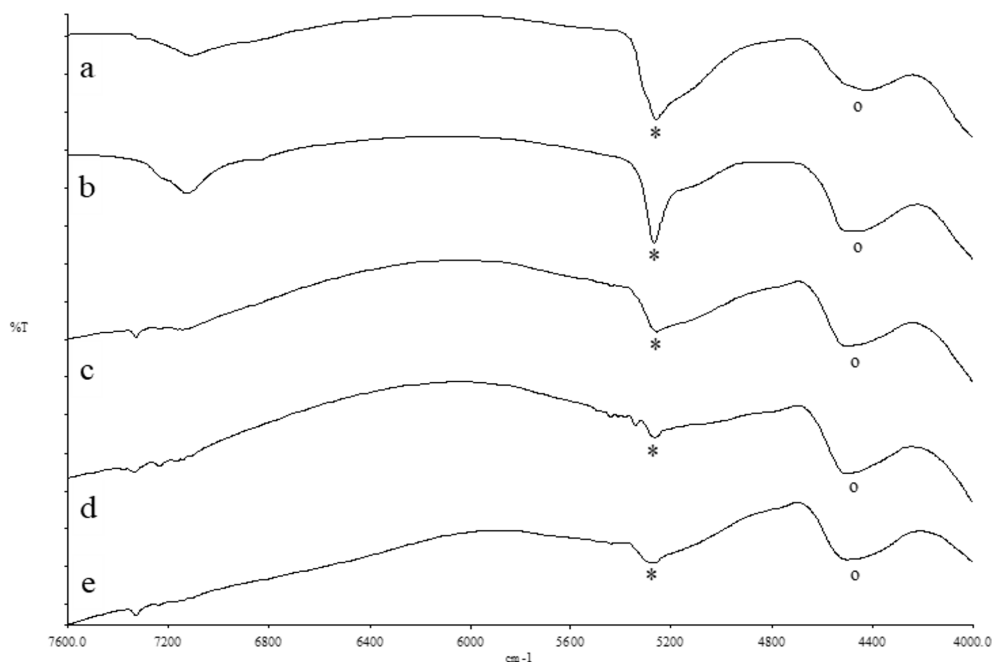
Figure 2. FT-NIRA partial spectra (7600-4000 cm-1) by Fraunhofer Approximation of different D50 (µm) silica samples. Marked bands: 4440 cm-1 (0) and 5268 cm-1 (*): a) MSS 500/3H (3.28); b) Chiffonsil-5 (4.87); c) Oristar Silica 7 (5.93); d) Silica Balloon BA4 (6.13); e) Silica HDK N20(16.46).

2008). This characteristic may cause errors in the quantitative methodology.

Samples with differences in D50 values were also not used to avoid falling within the experimental error. Analysis priority was given to lower D50 silica plates (HPTLC), in comparison with TLC, in order to investigate if the quantitative methodology was able to differentiate these two types.

DRIFT/MIR quantitative methodology

The silica characteristic band around 1060 cm-1 was analyzed in order to assess whether this band would be the most appropriate analytical band for the analysis of a larger number of samples. If acceptable, it would respond to the adopted DRIFT/MIR methodology, displayed in Table V. Figure 3 shows the DRIFT/MIR calibration curve (A1060) *versus* to the D50 values measured by the Fraunhofer Approximation (Equation 5).

From both Table V and Figure 3 it can be inferred that the samples satisfactorily responded to the DRIFT methodology (A1060).

$$y = 0.2261 + 0.01663\ x \qquad\qquad (5)$$

where y is the analytic band median (A1060) and x is the silica particle D50 measured by Fraunhofer diffraction method.

The calibration curve equation, Equation 5, indicates a good linearity (R = 0.960). 92% (R2 = 0.922) of the data can be explained by the methodology, with a 3.01% methodology error, which is considered satisfactory within the conditions of analysis. Since the error is relatively close to the reference value, ≤ 2% (Hórak & Vítek 1978), it can be considered satisfactory. Therefore, it is an indication that the methodology can meet the goal. The reference value is commonly found in conditions with less variation in the optical path/thickness, that is, liquid sample analyzed by transmission/closed or sealed cell. Furthermore, it is a much smaller error than that found in transmission/pellet powders quantitative analysis (around 8-10%) (Smith 1979) or in silica particle size determination by sedimentation (10%) (Domínguez et al. 2020).

Table V. Data from the DRIFT / MIR methodology (A$_{1060}$) for silica samples, with data from D50 measured by the Fraunhofer Approximation.

| Sample (D50 – μm)	A$_{1060}$	A$_{1060}$ (median)	Standard deviation	Relative deviation (%)
MSS 500 (3.28)	0.291	0.272	0.007	2.57
	0.272			
	0.277			
	0.254			
	0.267			
Chiffonsil-5 (4.87)	0.297	0.297	0.009	3.03
	0.312			
	0.304			
	0.267			
	0.273			
Silica balloon BA4 (6.13)	0.317	0.334	0.016	4.79
	0.386			
	0.305			
	0.334			
	0.368			
HPTLC plate silica (6.94)	0.365	0.365	0.011	3.01
	0.364			
	0.398			
	0.355			
	0.410			
TLC plate silica (11.4)	0.397	0.405	0.011	2.72
	0.405			
	0.353			
	0.408			
	0.407			

NIRA quantitative methodology

The band intensity ratio (A_{4440}/A_{5268}) was analyzed in order to assess whether it would be the most appropriate analytical band for a larger number of samples analysis that would respond to the implemented NIRA methodology, illustrated in Table VI. Figure 4 shows the NIRA calibration curve (A_{4440}/A_{5268}) corresponding to the D50 measured by Fraunhofer Approximation (Equation 6).

From Table VI and Figure 4 it can be inferred that the samples satisfactorily responded to the NIRA methodology (A_{4440}/A_{5268}).

$$y = 0.0947 + 0.0972\,x\,, \tag{6}$$

where, y is the relative band median (A_{4440}/A_{5268}) and x is the silica particle size (D50) measured by Fraunhofer Approximation.
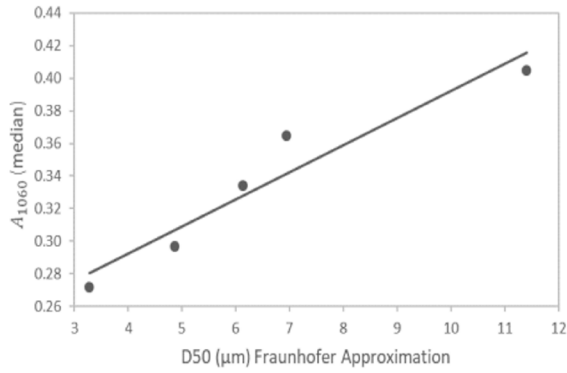
Figure 3. DRIFT/MIR calibration curve (A_{1060}) for silica D50 samples particle diameter calculation by Fraunhofer Approximation.
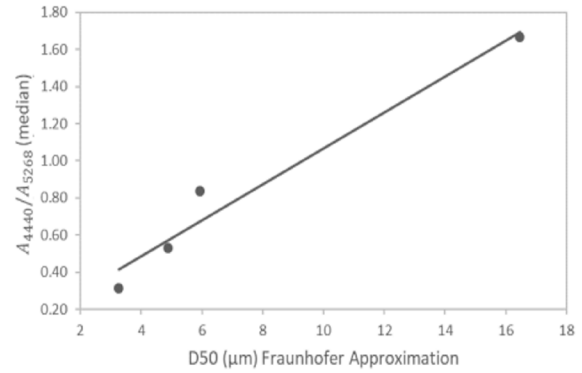
Figure 4. NIRA calibration curve (A_{4440}/A_{5268}) for silica samples particle diameter calculation D50 obtained by the Fraunhofer Approximation.

Table VI. NIRA methodology data (A_{4440}/A_{5268}) for silica samples, with D50 data measured by Fraunhofer Approximation.

Sample (D50 - μm)	A_{4440}	A_{5268}	A_{4440}/A_{5268}	A_{4440}/A_{5268} (median)	Standard deviation	Relative deviation (%)
MSS 500 (3.28)	0.056	0.179	0.313	0.313	0.004	1.28
	0.059	0.189	0.312			
	0.063	0.202	0.312			
	0.065	0.200	0.325			
	0.065	0.195	0.333			
CHIFFONSIL-5 (4.87)	0.085	0.162	0.525	0.531	0.002	0.38
	0.086	0.162	0.531			
	0.082	0.154	0.532			
	0.084	0.157	0.535			
	0.085	0.161	0.528			
Oristar Silica (5.93)	0.032	0.036	0.888	0.838	0.028	3.34
	0.031	0.039	0.795			
	0.03	0.036	0.833			
	0.031	0.037	0.838			
	0.03	0.032	0.938			
Silica HDK N20 (16.46)	0.034	0.018	1.888	1.666	0.108	6.48
	0.035	0.021	1.666			
	0.034	0.021	1.619			
	0.03	0.015	2.000			
	0.031	0.021	1.476			

The calibration curve equation, Equation 6, indicates good linearity (R = 0.981). 96% (R2 = 0.962) of data can be explained by the methodology, with a 2.31% methodology error, considered satisfactory within the analysis conditions, indicating that this methodology also can meet the goal.

The highest error observed in sample Silica HDK N20 is according to findings of literature, as shown in Table I, once it was found that samples of larger size of silica particles presented higher errors of absorbance values.

NIRA methodology effectiveness

Since NIRA methodology proved to be more appropriate to the determination, its effectiveness has been verified. To achieve this goal, a 4.88µm D50 silica sample, coded as "Sample A" was analyzed. The analysis was conducted according to the same conditions used for the elaboration of the corresponding calibration curve (Equation 6). Table VII shows the results of Equation 6 applied on the band intensity ratio (A_{4440}/A_{5268}). The obtained results, as expected, are close to the D50 value obtained by the granulometric analysis and are determined with an error around 2%.

Among the analyzed silica samples, the results confirm that the NIRA methodology is more adequate than the DRIFT for D50 determination. Even considering all the available

conditions such as samples characteristics and spectrum obtaining modes with more accurate data for smaller particle sizes, the results were validated.

However, other types of FTIR reflection techniques such as attenuated total reflectance (ATR) or universal attenuated total reflectance (UATR), can also be exploited in future publications.

CONCLUSION

Silica samples of different particle sizes were analyzed as received by DRIFT/MIR and NIRA. For DRIFT/MIR methodology, the band at 1060 cm-1 was evaluated. For NIRA methodology, the band intensity ratio (A4440/A5268) was evaluated.

For both methodologies, results show a tendency to smaller errors to in the absorbance measurements of samples with smaller or intermediate particle sizes, consistently with the literature data.

The criteria used to choose the most appropriate methodology for silica particles determination were the linearity (R), the percentage (%) of explained data (R2) and the evaluation of the methodology error. Both developed methodologies gave satisfactory results. However, the NIRA methodology showed a better linearity trend (R = 0.981) with approximately 96% of data explained by the

Table VII. Data related to NIRA methodology applied to the silica test sample.

Sample (D50) (by Fraunhofer approximation)	A4440	A5268	A4440/A5268	A4440/A5268 (median)	Standard deviation	Relative deviation (%)	D50 (µm) (by the methodology)
SILICA A (4.88)	0.072	0.142	0.507	0.526	0.007	1.33	4.44
	0.076	0.141	0.539				
	0.080	0.153	0.523				
	0.082	0.156	0.526				
	0.084	0.154	0.545				

developed methodology, and an error of 2.31%. Hence, it was possible to conclude that it proved to be more appropriate to the silica particle size determination with D50 data measurement acquired by Fraunhofer Approximation, a granulometric method that showed the best result, with less uncertainty and methodology error.

A parameter that suggests NIRA methodology can meet the objective is the 2.31% error. Since the error is relatively close to the reference value, ≤ 2%, it can be considered satisfactory. In addition, it also is a much smaller error than that found in powders quantitative analysis by transmission/pellet (8-10%) or by other sedimentation method for silica particles size determination (10%).

NIRA methodology effectiveness was demonstrated through the analysis of a silica test sample, under the same conditions used for the corresponding calibration curve elaboration. The results were close to the D50 values determined by the granulometric analysis (Fraunhofer diffraction method), with a relative error of 2%, approximately, within the equipment precision limits.

Acknowledgments

REFERENCES

ALAEI MH, MAHAJAN P, BRIEU M, KONDO D, RIZVI SJA, KUMAR S & BHATNAGAR N. 2013. Effect of particle size on thermomechanical properties of particulate polymer composite. Iran Polym 22: 853-863.

AMOABENG D, TEMPALSKI A, YOUNG BA, BINKS BP & VELANKAR SS. 2020. Fumed silica induces co-continuity across a wide composition range in immiscible polymer blends. Polym 186: 121831.

ARAI K, MIZUTANI T, MIYAMOTO M, KIMURA Y & AOKI T. 2019. Colloidal silica bearing thin polyacrylate coat: A facile inorganic modifier of acrylic emulsions for fabricating hybrid films with least aggregation of silica nanoparticles. Prog Org Coat 128: 11-20.

AZEVEDO JB, MURAKAMI LMS, FERREIRA AC, DINIZ MF, SILVA LM & DUTRA RCL. 2018. Quantification by FT-IR (UATR/NIRA) of NBR/SBR blends. Polimeros 28: 440-449.

BAHRANI S, GHAEDI M & DANESHFAR A. 2018. Fabrication of size controlled nanocomposite based on zirconium alkoxide for enrichment of Gallic acid in biological and herbal tea samples. J Chromatogr B Biomed Sci Appl 1087: 14-22.

BARTHEL H, RÖSCH L & WEIS J. 1996. Fumed Silica Production, Properties, and Applications, Organosilicon Chemistry Set: From Molecules to Materials. In: Auner N & Weis J (Eds), Organosilicon Chemistry Set, p. 761-778.

BASRUR A & SABDE D. 2016. Catalyst Synthesis and Characterization. In: Sunil SJ & Vivek VR (Eds), Industrial Catalytic Processes for Fine and Specialty Chemicals, Elsevier, p. 113-186.

BHEEKHUN N, TALIB ARA & HASSAN MR. 2013. Aerogels in Aerospace: An Overview. Adv Mater Sci Eng 2013: 406065.

BOLDYREV D, DEMA R & KALUGINA O. 2019. Research of Phase Composition of Graphitizing Ferro Silicon Barium Inoculants. Mater Today Proc 11: 510-515.

BRAY DJ, DITTANET P, GUILD FJ, KINLOCH AJ, MASANIA K, PEARSON RA & TAYLOR AC. 2013. The modelling of the toughening of epoxy polymers via silica nanoparticles: The effects of volume fraction and particle size. Polymer 54: 7022-7032.

BULATOVIC SM. 2015. Beneficiation of Silica Sand. In: Bulatovic SM (Ed), Handbook of Flotation Reagents: Chemistry, Theory and Practice, Petersborough: Elsevier, Ontario, CAN, p. 121-127.

BUTOV OV, GOLANT KM, TOMASHUK AL, VAN STRALEN MJN & BREULS AHE. 2002. Refractive index dispersion of doped silica for fiber optics. Opt Commun 213: 301-308.

BUTTRESS AJ, RODRIGUEZ JM, URE A, FERRARI RS, DODDS C & KINGMAN SW. 2019. Production of high purity silica by microfluidic-inclusion fracture using microwave pre-treatment. Miner Eng 131: 407-419.

CABASSI G, CAVALLI D, FUCCELLA R & GALLINA PM. 2015. Evaluation of four NIR spectrometers in the analysis of cattle slurry. Biosyst Eng 133: 1-13.

CAMPBELL JH ET AL. 2004. NIF optical materials and fabrication technologies: an overview. In: Lasers and Applications in Science and Engineering, San Jose. Proceedings v. 5341, Optical Engineering at the Lawrence Livermore National Laboratory II: The National Ignition Facility, San Jose.

CAMPOS EA, DUTRA RCL, REZENDE LC, DINIZ MF, NAWA WMD & IHA K. 2010. Performance evaluation of commercial copper chromites as burning rate catalyst for solid propellants. J Aerosp Technol Manag 2: 323-330.

CARVALHO TA, GAMA AC, MAGALHÃES RF, DINIZ MF, SANCHES NB & DUTRA RCL. 2021. Determination of nitrogen and acrylic / styrene components in nitrocellulose systems by UATR and NIRA infrared techniques. Polym Test 93: 106962.

CHEN JJ, NG PL, LI LG & KWAN AKH. 2017. Production of High-performance Concrete by Addition of Fly Ash Microsphere and Condensed Silica Fume. Procedia Eng 172: 165-171.

DA SILVA LM. 2013. A fabricação de pneus com sílica. UEZO, Rio de Janeiro, http://www.uezo.rj.gov.br/tcc/tp/Laerte-Mello-da-Silva.pdf. Accessed on Aug 13, 2021.

DAI S, PAN X, MA L, HUANG X, DU C, QIAO Y & WU Z. 2018. Discovery of the Linear Region of Near Infrared Diffuse Reflectance Spectra Using the Kubelka-Munk Theory. Front Chem 6: 154.

DAI Z, XIE X, ZHOU L, CHEN S & GAN Z. 2019. Investigation of global thermal effect of large fused silica surface figuring using inductively coupled plasma. Optik 180: 254-263.

DOMÍNGUEZ JMA, RAMAYE Y, DABRIO M & KESTENS V. 2020. Validation of a Homogeneous Incremental Centrifugal Liquid Sedimentation Method for Size Analysis of Silica (Nano)particles. Materials 13: 3806.

DUDEK M, KABAŁA C, ŁABAZ B, MITUŁA P, BEDNIK M & MEDY´NSKA-JURASZEK A. 2021. Mid-Infrared Spectroscopy Supports Identification of the Origin of Organic Matter in Soils. Land 10: 1-11.

DUTRA RCL & SOARES BG. 1998. Determination of the vinyl mercaptoacetate contente in poly(ethylene-co-vinyl acetate-co-vinyl mercaptoacetate) (EVASH) by TGA analysis and FTIR spectroscopy. Polym Bull 41: 61-67.

ELSAYED H, PICICCO M, DASAN A, KRAXNER J, GALUSEK D & BERNARDO E. 2019. Glass powders and reactive silicone binder: Interactions and application to additive manufacturing of bioactive glass-ceramic scaffolds. Ceram Int 45: 13740-13746.

FERRÃO MF. 2001. Técnicas de Reflexão no Infravermelho Aplicadas na Análise de Alimentos. Tecnológica 5: 65-85.

FERREIRA AC, DINIZ MF, FERREIRA ACB, SANCHES NB & MATTOS ECM. 2020. FT-IR/UATR and FT-IR transmission quantitative analysis of PBT/PC blends. Polym Test 85: 106447.

FRENI A, CALABRESE L, MALARA A, FRONTERA P & BONACCORSI L. 2019. Silica gel microfibres by electrospinning for adsorption chillers. Energy 187: 115971.

FULLER MP & GRIFFITHS PRMP. 1978. Diffuse reflectance measurements by infrared Fourier transform spectrometry. Anal Chem 50: 1906-1910.

GAO Q, WU X, XIA Z & FAN Y. 2017. Coating mechanism and near-infrared reflectance property of hollow fly ash bead/TiO2 composite pigment. Powder Technol 305: 433-439.

GODDU RF. 1960. Near-Infrared spectrophotometry. In: Reilly CN (Ed), Advances in analytical chemistry and instrumentation, New York: Interscience, p. 347-425.

GOMES MM. 1993. Polímeros/Elastômeros/Borrachas. Borracha Nitrilica (NBR) (1993). Retrieved from: < http://www.rubberpedia.com/borrachas/borracha-nitrilica.php> Accessed on 16 jun. 2020.

GÜRGEN S. 2019. Wear performance of UHMWPE based composites including nano-sized fumed sílica. Compos B Eng 173: 106967.

GUTIÉRREZ-CASTORENA MC & EFFLAND WR. 2010. Pedogenic and Biogenic Siliceous Features. In: Stoops G, Marcelino V & Mees F (Eds), Interpretation of Micromorphological Features of Soils and Regoliths, Elsevier, p. 471-496.

HALIM ZAA, YAJID MAM, IDRISM H & HAMDAN H. 2017. Effects of silica aerogel particle sizes on the thermal-mechanical properties of silica aerogel - unsaturated polyester composites. Plast Rubber Compos Macro Eng 46: 184-192.

HOPKINSON L, RUTT KJ & KRISTOVA P. 2018. The near-infrared spectra of the alkali carbonates. Spectrochim Acta A Mol Biomol Spectrosc 200: 143-149.

HÓRAK MA & VÍTEK A. 1978. Interpretation and Processing of Vibrational Spectra. New York: J Wiley & Sons, 414 p.

JANZEN DA, DINIZ MF, AZEVEDO JB, PINTO JRA, SANCHES NB & DUTRA RCL. 2021. Qualitative And Quantitative Evaluation Of Epoxy Systems By Fourier Transform Infrared Spectroscopy And The Flexibilizing Effect Of Mercaptans. An Acad Bras Cienc 93: e20200799.

KARNATI SR, AGBO P & ZHANG L. 2020. Applications of silica nanoparticles in glass/carbon fiber-reinforced epoxy nanocomposite. Compos Commun 17: 32-41.

KESTENS V ET AL. 2016. Challenges in the size analysis of a silica nanoparticle mixture as candidate certified reference material. J Nanopart Res 18: 1-22.

KONG J, SUN J, TONG Y, DOU Q, WEI Y, THITSARTARN W, YEO JCC & HE C. 2019. Carbon nanotubes-bridged-fumed silica as an effective binary nanofillers for reinforcement of silicone elastomers. Compos Sci Technol 169: 232-241.

KORTE EH. 1988. Figures of Merit for a Diffuse Reflectance Accessory Using an On-Axis Ellipsoidal Collecting Mirror. Appl Spectrosc 42: 428-433.

LEI H, LIU T & XU L. 2019. Synthesis of Sm-doped colloidal SiO2 composite abrasives and their chemical mechanical polishing performances on sapphire substrates. Mater Chem Phys 237: 121819.

LU Z, XU L, HE Y & ZHOU J. 2019. One-step facile route to fabricate functionalized nano-silica and silicone sealant based transparent superhydrophobic coating. Thin Solid Films 692: 137560.

MAGALHÃES RF, BARROS AL, TAKEMATSU MM, SANCHES NB, QUAGLIANO JCA & DUTRA RCL. 2020. FT-IR surface analysis of poly [(4-hydroxybenzoic)-ran-(2-hydroxy-6-naphthoic acid)] fiber - A short review. Polym Test 90: 106750.

MARTINS PFF. 2016. Obtenção de sílica de elevada pureza a partir do rejeito de flotação de um minério itabirítico. Doctoral Thesis, Postgraduate Program in Radiation, Minerals and Materials Science and Technology. Nuclear Technology Development Center, Belo Horizonte, Brazil, 128 p.

MCNAB AI, MCCUE AJ, DIONISI D & ANDERSON JA. 2017. Quantification and qualification by in-situ FTIR of species formed on supported-cobalt catalysts during the Fischer-Tropsch reaction. J Catal 353: 286-294.

MELLO TSD, DINIZ MF & DUTRA RCL. 2018. UATR and NIRA evaluation in the quantification of ATBC in NC blends. Polímeros 28: 239-245.

NAI-NING W, HANG -JIAN Z & XIAN-HUANG YU. 1992. A versatile Fraunhofer diffraction and Mie scattering based laser particle sizer. Adv Powd Technol 3: 7-14.

OSBORNE BG. 2000. Near-Infrared Spectroscopy in Food Analysis. In: Meyers RA (Ed), Encyclopedia of Analytical Chemistry, J Wiley & Sons, 1434 p.

OSSWALD J & FEHR KT. 2006. FTIR spectroscopic study on liquid silica solutions and nanoscale particle size determination. J Mater Sci 41: 1335-1339.

OZAKI Y. 2012. Near-Infrared Spectroscopy - Its Versatility in Analytical Chemistry. Anal Sci 28: 545-563.

PAIVA AA & GARBELOTTO PR. 2006. Formulação de borracha de epdm reforçada com sílica precipitada, processo para sua fabricação, processo para obtenção de um perfil de borracha reforçada, perfil de borracha extrudado colorido e uso de formulação de borracha reforçada. Patent PI 0501490-5 A2 Rhodia Brasil Ltda.

PERKINELMER. 2011. IR ready for any challenge. Retrieved from: <https://www.perkinelmer.com/lab.../docs/BRO_FrontierFTIR.pdf>. Accessed on 10 Oct. 2017.

PHUA EJR, LIU M, CHO B, LIU Q, AMINI S, HU X & GAN CL. 2018. Novel high temperature polymeric encapsulation material for extreme environment electronics packaging. Mater Des 141: 202-209.

PINTO JRA, SANCHES NB, DINIZ MF, SANTOS RS, OLIVEIRA JIS & DUTRA RCL. 2018. Expanded perlite/cork fillers applied to aerospace insulation materials. An Acad Bras Cienc 90: 3197-3206.

RAJAEE P, GHASEMI FA, FASIHI M & SABERIAN M. 2019. Effect of styrene-butadiene rubber and fumed silica nano-filler on the microstructure and mechanical properties of glass fiber reinforced unsaturated polyester resin. Compos B Eng 173: 106803.

RAMALHO FMG, SIMETTI R, ARRIEL TF, LOUREIRO BA & HEIN PRG. 2019. Influence of Particles Size on NIR Spectroscopic Estimations of Charcoal Properties. Flor Ambient 26: e20180397.

RIGOLI PS, MURAKAMI LMS, DINIZ MF, AZEVEDO MFP, CASSU SN, MATTOS EC & DUTRA RCL. 2019. Quantification of Aerospace Polymer Blends by Thermogravimetric Analysis and Infrared Spectrometry. J Aerosp Technol Manag 11: 1-12.

ROGGO Y, CHALUS P, MAURER L, LEMA-MARTINEZ C, EDMOND A & JENT N. 2007. A review of near infrared spectroscopy and chemometrics in pharmaceutical technologies. J Pharm Biomed Anal 44: 683-700.

SAHU O & SINGH N. 2019. Significance of bioadsorption process on textile industry wastewater. In: Shahid-Ul-Islam & Butola BS (Eds), The Impact and Prospects of Green Chemistry for Textile Technology, Woodhead Publishing, p. 367-416.

SATTAYANURAK S, SAHAKARO K, KAEWSAKUL W, DIERKES WK, REUVEKAMP LAEM, BLUME A & NOORDERMEER JWM. 2020. Synergistic effect by high specific surface area carbon black as secondary filler in silica reinforced natural rubber tire tread compounds. Polym Test 81: 106173.

SCHILL W, HEYDEN S, CONTI S & ORTIZ M. 2018. The anomalous yield behavior of fused silica glass. J Mech Phys Solids 113: 105-125.

SHARMA J & POLIZOS G. 2020. Hollow Silica Particles: Recent Progress and Future Perspectives. Nanomaterials 10: 1-22.

SHARMA DK, SHARMA A & TRIPATHI SM. 2018. Thermo-optic Characteristics of hybrid polymer/silica microstructured optical fiber: An analytical approach. Opt Mater 78: 508-520.

SHEPPARD RY, MILLIKEN RE, RUSSELL JM, DYAR MD, SKLUTE EC, VOGEL H, MELLES M, BIJAKSANA S, MORLOCK MA & HASBERG AKM. 2019. Characterization of Iron in Lake Towuti sediment. Chem Geol 512: 11-30.

SHI X, PAN G, ZHOU Y, GU Z, GONG H & ZOU C. 2014. Characterization of colloidal silica abrasives with different sizes and their chemical-mechanical polishing performance on 4H-SiC (0001). Appl Surf Sci 307: 414-427.

SHIMADZU. 2020. Fraunhofer Diffraction Theory and Mie Scattering Theory. Retrieved from: <https://www.shimadzu.com/an/powder/support/practice/p01/lesson13.html.> Accessed on May 29, 2020.

SIDDIQUE R & CHAHAL N. 2011. Use of silicon and ferrosilicon industry by-products (silica fume) in cement paste and mortar. Resour Conserv Recycl 55: 739-744.

SMITH AL. 1979 Applied Infrared Spectroscopy: Fundamentals Techniques and Analytical Problem-Solving, 1st ed., J Wiley & Sons, 336 p.

SÖZ CK, YILGÖR E & YILGÖR I. 2015. Influence of the coating method on the formation of superhydrophobic silicone-urea surfaces modified with fumed silica nanoparticles. Prog Org Coat 84: 143-152.

SRIRAM S, SINGH RK & KUMAR A. 2020. Silica and Silane based polymer composite coating on glass slide by dip-Coating Method. Surf Interfaces 19: 100472.

STACH R, BARONE T, CAUDA E, KREBS P, PEJCIC B, DABOSS S & MIZAIKOFF B. 2020. Direct infrared spectroscopy for the size-independent identification and quantification of respirable particles relative mass in mine dusts. Anal Bioanal Chem 412: 3499-3508.

TAGLIAFERRO FS, FERNANDES EN, BACCH MA, CAMPOS EA, DUTRA RCL & DINIZ MF. 2006. INAA for the validation of chromium and copper determination in copper chromite by infrared spectrometry. J Radioanal Nucl Chem 269: 403-406.

TAN C, ZHAO L, CHEN M, CHENG J, WU C, LIU Q, YANG H, YIN Z & LIAO W. 2020. Experimental and theoretical investigation of localized CO2 laser interaction with fused silica during the process of surface damage mitigation. Results Phys 16: 102936.

TANG H, YANG W, LIU W, MA J & LUO X. 2020. Characteristic of fixed abrasive polishing for fused silica in anhydrous environment. Optik 202: 163623.

TIAN M, YAO L, HAN A, ZHU X, CHEN C, YE M & CHEN X. 2020. Near-infrared reflectance and thermal insulating performance of Mo-doped Bi2WO6 with 3D hierarchical flower-like structure as novel ceramics pigment. Ceram Int 46: 12566-12573.

TORRENT J & BARRÓN V. 2008. Diffuse Reflectance Spectroscopy. In: Ulery AL & Drees RL (Eds), Methods of Soil Analysis Part 5—Mineralogical Methods, Madison : Soil Science Society of America, Wisconsin, USA, p. 367-385.

TWEDDLE D, HAMER P, SHEN Z, MOODY MP & WILSHAW PR. 2019. Identification of colloidal silica polishing induced contamination in silicon. Mater Charact 152: 239-244.

VUKCEVICH MR. 1972. A new interpretation of the anomalous properties of vitreous silica. J Non Cryst Solids 11: 25-63.

WAGNER DT & ARANHA IB. 2007. Método para análise de tamanho de partícula por espalhamento de luz para Bentonita Chocolate. In: XV Jornada de Iniciação Científica, Centro de Tecnologia Mineral, Rio de Janeiro, p. 1-8.

WILLIAMS P & NORRIS K. 2001. Near-Infrared Technology. 2nd ed., St. Paul: Amer Assn of Cereal Chemists, 312 p.

XU L, LEI H, WANG T, DONG Y & DAI S. 2019. Preparation of flower-shaped silica abrasives by double system template method and its effect on polishing performance of sapphire wafers. Ceram Int 45: 8471-8476.

ZAFARMEHRABIAN R, GANGALI ST, GHOREISHY MHR & DAVALLU M. 2012. The effects of silica/carbón black ratio on the dynamic properties of the tread compounds in track tires. Ejchem 9: 1102-1112.

ZHAO Q, LV X, JIA Y, CHEN Y, XU G & QU L. 2018. Rapid determination of the fat, moisture, and protein contents in homogenized chicken eggs based on near-infrared reflectance spectroscopy. Poult Sci 97: 2239-2245.

RACHEL F. MAGALHÃES[1]
https://orcid.org/0000-0002-1364-3748

ALEXANDRA H. DE BARROS[1]
https://orcid.org/0000-0001-0963-2885

MARCIA M. TAKEMATSU[1]
https://orcid.org/0000-0001-9323-3898

ALAN PASSERO[1]
https://orcid.org/0000-0003-1938-8458

MILTON F. DINIZ[2]
https://orcid.org/0000-0003-0246-0660

JAIRO SCIAMARELI[2]
https://orcid.org/0000-0001-8014-9603

RITA C.L. DUTRA[1]
https://orcid.org/0000-0001-9958-1279

[1]Instituto Tecnológico de Aeronáutica (ITA), Departamento
de Ciência e Tecnologia Aeroespacial (DCTA), Divisão
de Ciências Fundamentais, Departamento de Química,
Praça Marechal Eduardo Gomes, 50, Vila das Acácias,
12228-900 São José dos Campos, SP, Brazil

[2]Instituto de Aeronáutica e Espaço (IAE), Divisão de Propulsão,
Departamento de Ciência e Tecnologia Aeroespacial
(DCTA), Praça Marechal Eduardo Gomes, 50, Vila das
Acácias, 12228-904 São José dos Campos, SP, Brazil

Correspondence to: **Rita de Cássia Lazzarini Dutra**
E-mail: ritacld@ita.br

Author contributions

Conceptualization: Magalhães RF & Dutra RCL; Methodology: Magalhães RF, Barros AH, Takematsu MM, Passero A, Sciamareli J, Diniz MF & Dutra RCL; Investigation: Magalhães RF, Passero A, Diniz MF, Barros AH, & Sciamareli J; Writing - Original Draft: Magalhães RF & Dutra RCL; Writing - Review & Editing: Magalhães RF, Takematsu MM & Dutra R.C.L; Funding Acquisition: Dutra R.C.L; Resources: Takematsu MM & Passero A; Supervision: Magalhães RF, Takematsu MM. & Dutra RCL.